

An assessment of structural enthalpy and crystallization pathways of $\text{Mg}_{65}\text{Zn}_{30}\text{Ca}_5$ bulk metallic glass and amorphous films

Scott Gleason, David Miskovic, Nicholas Hamilton, Kevin Laws, Michael Ferry

UNSW Australia
School of Material Science and Engineering

July 26, 2017

ABSTRACT

The structural nature and thermal stability of amorphous alloys is highly dependent on the method by which they are produced, i.e. their relaxation rate upon cooling. Both bulk samples and metallic glass films of $\text{Mg}_{65}\text{Zn}_{30}\text{Ca}_5$ were produced by copper mold casting and direct current (DC) magnetron sputtering onto aluminium substrates, respectively. Comparisons between structural enthalpy, crystallization pathways, relaxation and crystallization kinetics of the bulk samples and films were examined by elevated temperature XRD and DSC. Compared with equivalent experiments on the bulk alloy, results for the thin films show distinct differences in structural enthalpy and deviations from the expected crystalline phase evolution, displaying minor peak shifts, failure of some phases to evolve, and variations in the evolution rates.

TABLE OF CONTENTS

ABSTRACT	i
TABLE OF CONTENTS	1
1 INTRODUCTION	1
2 METHOD	1
2.1 Master alloy	1
2.2 DC magnetron sputtering	1
2.3 DSC characterization	2
2.4 XRD characterization	2
3 RESULTS	2
4 DISCUSSION	3
5 CONCLUSIONS	3
6 ACKNOWLEDGEMENTS	3
7 REFERENCES	3

1 INTRODUCTION

The structural nature and thermal stability of amorphous alloys is highly dependent on the method by which they are produced, i.e. their relaxation rate upon cooling. Both bulk samples and metallic glass films of $\text{Mg}_{65}\text{Zn}_{30}\text{Ca}_5$ were produced by copper mold casting and direct current (DC) magnetron sputtering onto aluminium substrates, respectively. Comparisons between structural enthalpy, crystallization pathways, relaxation and crystallization kinetics of the bulk samples and films were examined by elevated temperature XRD and DSC. Compared with equivalent experiments on the bulk alloy, results for the thin films show distinct differences in structural enthalpy and deviations from the expected crystalline phase evolution, displaying minor peak shifts, failure of some phases to evolve, and variations in the evolution rates.

Key sources [\[1, 2\]](#) [\[3\]](#) [Zhang Zhang Zhang 2012](#)

2 METHOD

2.1 Master alloy

The master alloy of $\text{Mg}_{65}\text{Zn}_{30}\text{Ca}_5$ was produced using high-purity elements of Mg (99.85 wt%), Zn (99.995 wt%), and Ca (99.8 wt%). The alloy was prepared by induction melting in boron nitride coated graphite crucibles, purged with Ar (99.997 vol.% purity) five times, and protected with a circulating Ar atmosphere. Alloy homogeneity was ensured through heating and cooling through a cycle 700°C, 385°C, 650°C, 385°C, 650°C to a casting temperature of 500 °C and 450°C for for injection and gravity casting respectively. Bulk amorphous $\text{Mg}_{65}\text{Zn}_{30}\text{Ca}_5$ plate with a thickness of $XX\mu\text{m}$ was produced by copper mold injection casting. The 25.4mm diameter targets were prepared from a cylindrical copper mold gravity casting sectioned to thicknesses of 3.25mm.

2.2 DC magnetron sputtering

Films were produced from an in-house DC magnetron sputtering facility with Ar working gas (99.997 vol.% purity). The power was 15W, typical voltage of 290 – 350V, nominal chamber temperature of 25 °C, pressure 1 bar, Ar flow 3.01 standard cubic centimetres per minute (SCCM).

2.3 DSC characterization

DSC

2.4 XRD characterization

Annealing XRD (PANalytical Empyrean) with a Cu K_α X-ray source ($\lambda = 1.541\text{\AA}$). Generator Voltage 45, Tube Current 40, Scan Step Size 0.0262606, Time per step 397.29.

Dynamic XRD (Bruker D8) with a Cu K_α X-ray source ($\lambda = 1.541\text{\AA}$). Generator Voltage 45, Tube Current 100, Scan Step Size 0.02, Time per step 134.4.

XRD heated in 5 degree increments at 20 k/min. scans of xx over a range of 31 - 60 2 theta allows 20 minute scans.

3 RESULTS

deposition were for 35 minutes, and saw an average temperature rise of 3 – 4 °C during the deposition. Nominal film thickness was about $2.5\mu\text{m}$ giving a deposition rate of 1.2nm/s .

Relaxed differential scanning calorimetry (DSC) of bulk material taken at different heating rates was used to establish the fragility of the $\text{Mg}_{65}\text{Zn}_{30}\text{Ca}_5$ system. From the equations ... a fit of $\beta^{-1} = 1.338E - 16e^{5274(\frac{1}{T-T_0})}$ with Adj. $R^2 = 0.972$ was established. This give a $D^* = 20.4$ which using $D^* = 590/(m - 16)$ Shuai2014 [4, 5] gives a fragility $m = 44.9$.

Heating Rate β K/min	T_g	T_{x1}	T_{x2}	T_{x3}	T_{x4}	T_{x5}
100	136.1	163.4	205.2	217.2	251.2	270.6
80	132.0	159.5	201.5	213.7	245.3	266.0
60	129.6	157.4	199.1	210.9	240.6	261.8
40	126.6	155.0	196.3	208.0	234.8	256.3
30	126.2	151.1	193.7	204.8	230.5	252.3
20	125.1	149.8	190.9	201.4	224.1	247.5
15	123.8	148.5	189.2	199.3	220.7	244.4
10	123.5	144.7	186.1	195.9	215.4	240.2
5	120.5	141.7	181.9	189.8	204.5	232.8

Table 1: Bulk $\text{Mg}_{65}\text{Zn}_{30}\text{Ca}_5$ alloy onset temperatures for the various DSC heating rates β . All temperatures are in °C.

4 DISCUSSION

The use of a 60K DSC heating rate compared to the more commonly used 20K rate [sources] shifts peaks for the bulk $\text{Mg}_{65}\text{Zn}_{30}\text{Ca}_5$ alloy about 8 - 15 degrees higher. This higher heating rates were used because crystallization events for the films were different to differentiation at the lower heating rate. Films show little shift to high temperature peaks with increases heating rates, but large shifts with relaxation. Bulk show the opposite behaviour, larger peaks shifts with higher heating rates and little shift with relaxation.

5 CONCLUSIONS

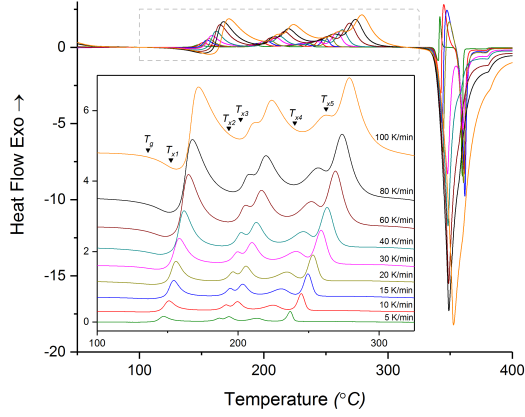
6 ACKNOWLEDGEMENTS

Yu Wang for his assistance with XRD experimentation and Rietveld refinement.

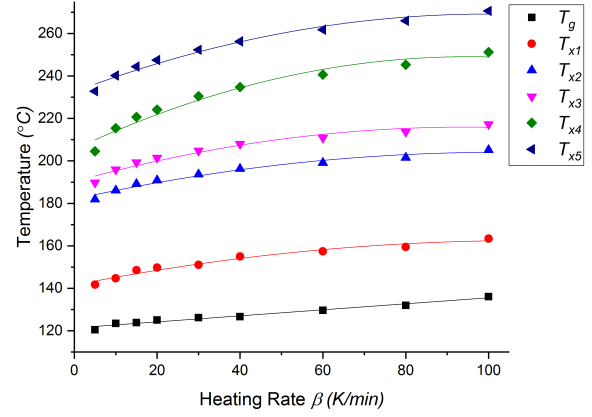
7 REFERENCES

- hang2013 [1] Y. N. Zhang, G. J. Rocher, B. Briccoli, D. Kevorkov, X. B. Liu, Z. Altounian, and M. Medraj. Crystallization characteristics of the Mg-rich metallic glasses in the Ca-Mg-Zn system. *Journal of Alloys and Compounds*, 552:88–97, 2013.
- hang2012 [2] Yi-Nan Zhang, Dmytro Kevorkov, Xue Dong Liu, Florent Bridier, Patrice Chartrand, and Mamoun Medraj. Homogeneity range and crystal structure of the $\text{Ca}_2\text{Mg}_5\text{Zn}_{13}$ compound. *Journal of Alloys and Compounds*, 523:75–82, 2012.
- hang2011 [3] Yi-Nan Zhang, Dmytro Kevorkov, Florent Bridier, and Mamoun Medraj. Experimental study of the Ca-Mg-Zn system using diffusion couples and key alloys. *Science and Technology of Advanced Materials*, 12(2):025003, 2011.
- Cao2013 [4] Jake Diablo Cao. Processing and properties of biocompatible metallic glasses, 2013.
- Cao2012 [5] J D Cao, K J Laws, N Birbilis, and M Ferry. Potentiodynamic polarisation study of bulk metallic glasses based on the Mg-Zn-Ca ternary system. *Corrosion Engineering, Science and Technology*, 47(5):329–334, 2012.
- Gu2005 [6] X. Gu, G.J. Shiflet, F.Q. Guo, and S.J. Poon. Mg-Ca-Zn bulk metallic glasses with high strength and significant ductility. *Journal of Materials Research*, 20(08):1935–1938, 2005.

- Zhou2013 [7] X. Zhou, K. D. Ralston, K. J. Laws, J. D. Cao, R. K. Gupta, M. Ferry, and N. Birbilis. Effect of the degree of crystallinity on the electrochemical behavior of $\text{Mg}_{65}\text{Cu}_{25}\text{Y}_{10}$ and $\text{Mg}_{70}\text{Zn}_{25}\text{Ca}_5$ bulk metallic glasses. *Corrosion*, 69(8):781–792, 2013.
- Wang2013 [8] Jingfeng Wang, Song Huang, Yang Li, Yiyun Wei, Xingfeng Xi, and Kaiyong Cai. Microstructure, mechanical and bio-corrosion properties of Mn-doped Mg-Zn-Ca bulk metallic glass composites. *Materials Science and Engineering: C*, 33(7):3832–3838, 2013.

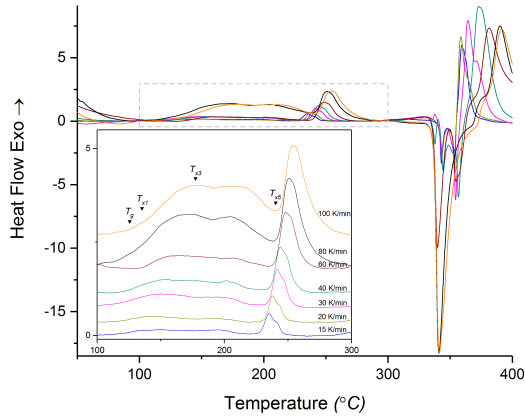


(a) fig:DSC_Onsets_Bulk

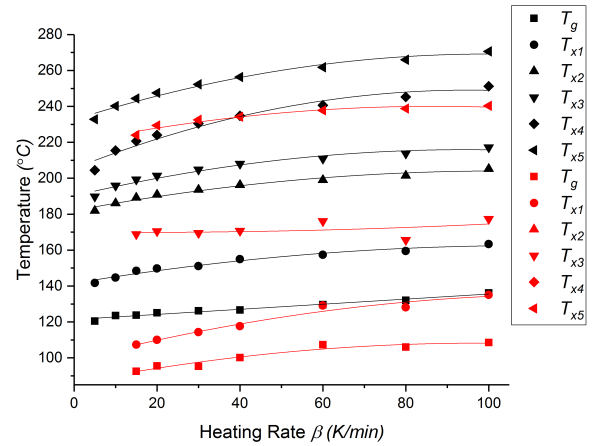


(b)

Figure 1: (a) Bulk $\text{Mg}_{65}\text{Zn}_{30}\text{Ca}_5$ relaxed at 120 °C for 10 minutes and heated at various heating rates. The insert stacks the DSC curves and labels the T_g and T_x es of the 100K/min sample. (b) The T_g s and T_x es of the bulk $\text{Mg}_{65}\text{Zn}_{30}\text{Ca}_5$ at all heating rates.



(a) fig:DSC_Onsets_Film



(b)

Figure 2: (a) Unrelaxed film $\text{Mg}_{65}\text{Zn}_{30}\text{Ca}_5$ heated at various heating rates. The insert stacks the DSC curves and labels the T_g and T_x es of the 100K/min sample. (b) The T_g s and T_x es of the bulk and film $\text{Mg}_{65}\text{Zn}_{30}\text{Ca}_5$ at all heating rates.

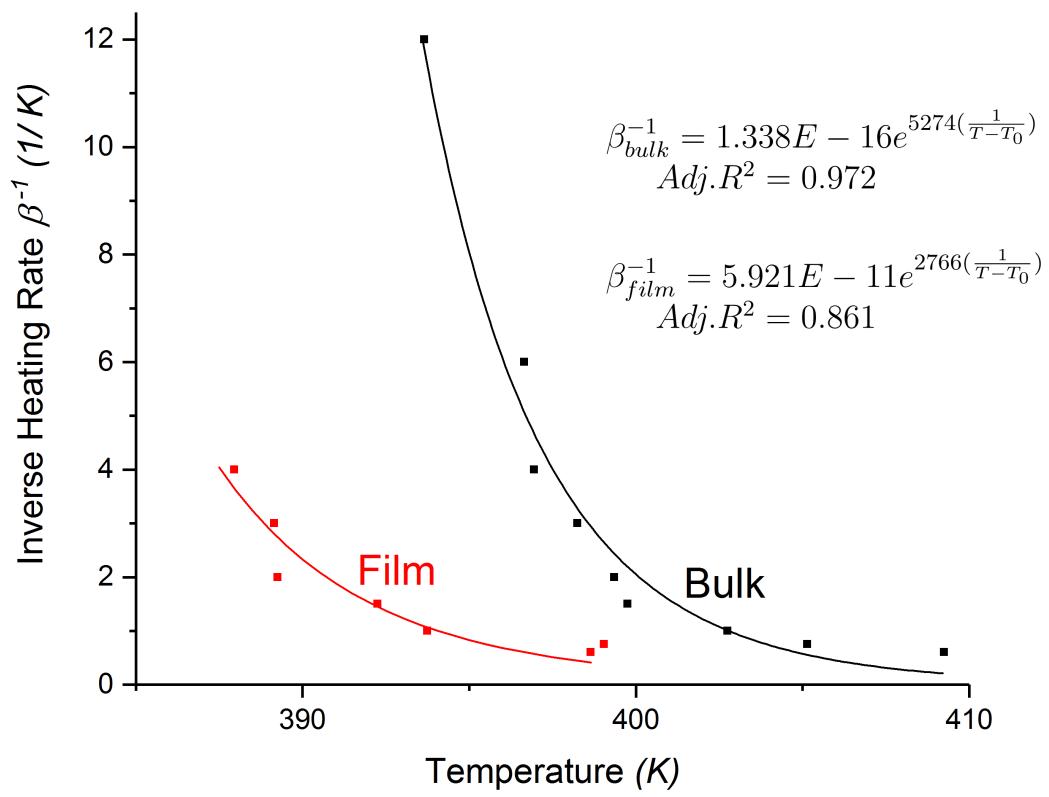
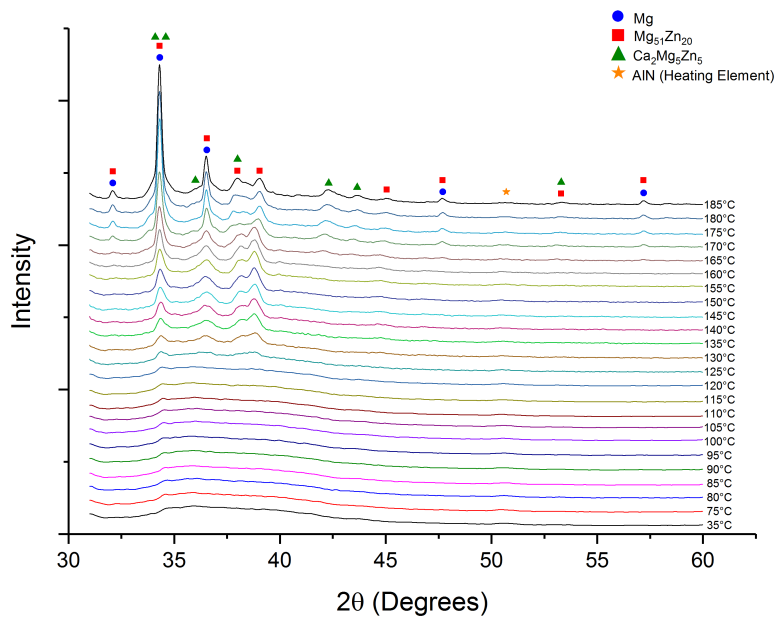
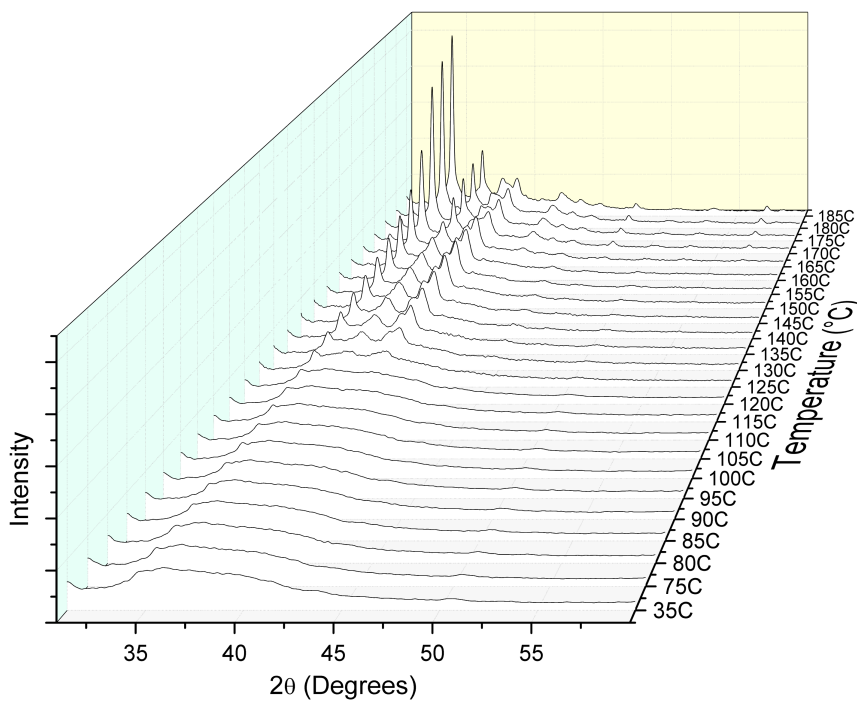


Figure 3: Fitted fragility for the $Mg_{65}Zn_{30}Ca_5$ system obtained by DSC at various heating rates

m_mValue

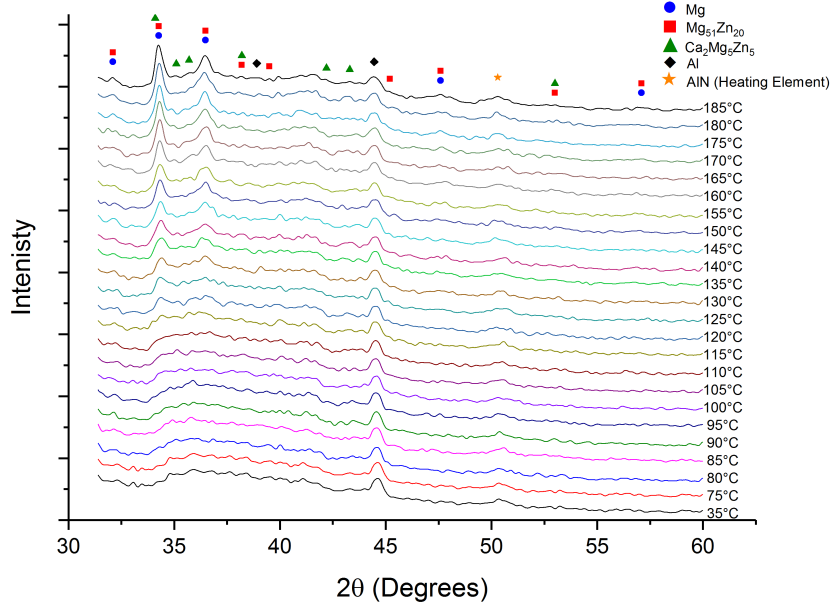


(a)

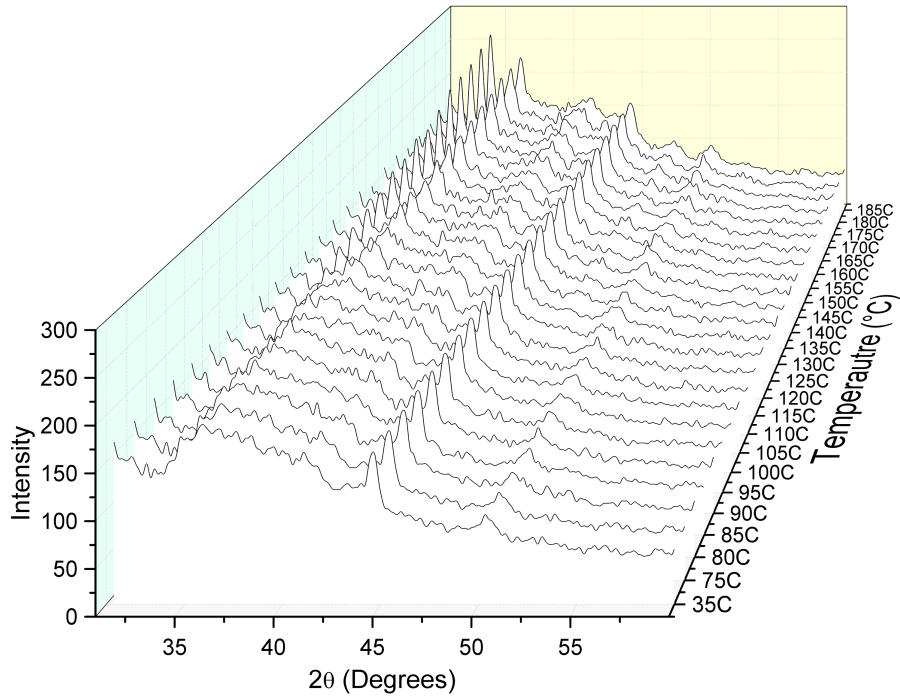


(b)

Figure 4: (a) Stacked X-ray diffraction (XRD) patterns from the incremental heating of bulk $\text{Mg}_{65}\text{Zn}_{30}\text{Ca}_5$. (b) Cascading XRD patterns from the incremental heating of bulk $\text{Mg}_{65}\text{Zn}_{30}\text{Ca}_5$.



(a)



(b)

Figure 5: (a) Stacked XRD patterns from the incremental heating of film $\text{Mg}_{65}\text{Zn}_{30}\text{Ca}_5$. (b) Cascading XRD patterns from the incremental heating of film $\text{Mg}_{65}\text{Zn}_{30}\text{Ca}_5$.

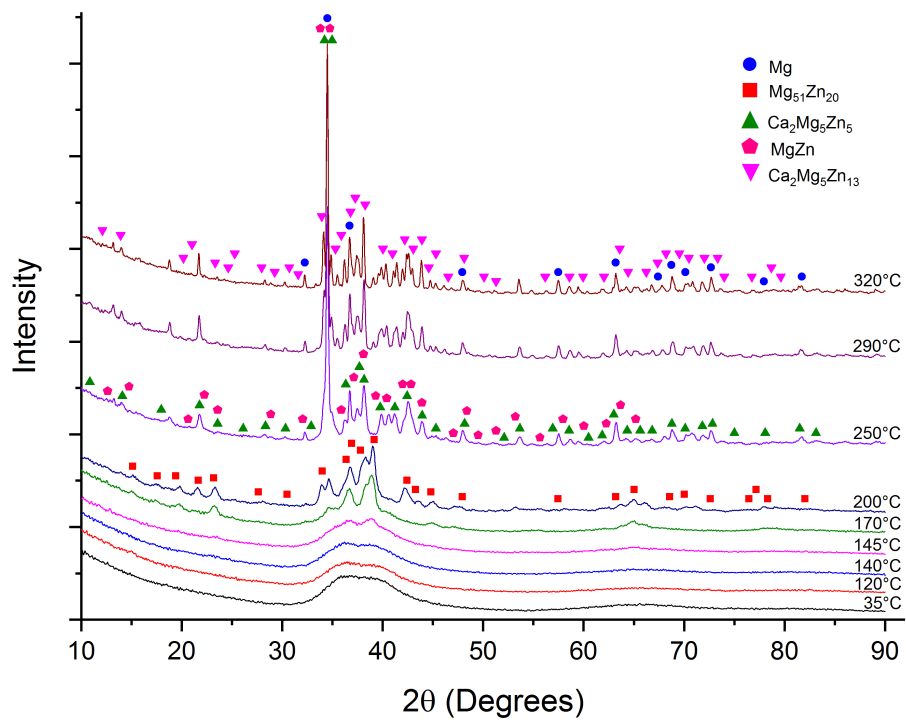


Figure 6: XRD pattern for Bulk $\text{Mg}_{65}\text{Zn}_{30}\text{Ca}_5$ heated through several crystallization peaks identified from DSC

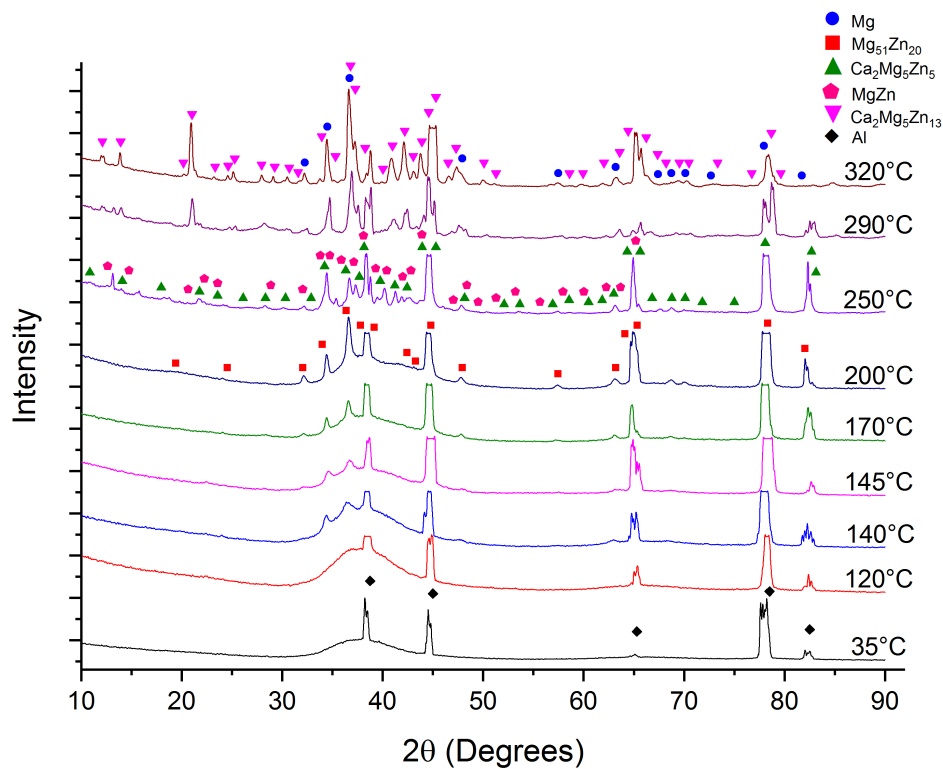


Figure 7: XRD pattern for Film $\text{Mg}_{65}\text{Zn}_{30}\text{Ca}_5$ heated through several crystallization peaks identified from DSC